

1 **Pre-Columbian treponemes clarify worldwide spread of**
2 **treponematosis**

3

4 GUEYRARD Mattéo¹⁻², PONTAROTTI Pierre¹⁻³, DRANCOURT Michel¹⁻², ABI-RACHED Laurent^{1-3,*}

5

6 1: Aix Marseille Univ., IRD, MEPHI, AP-HM, IHU-Méditerranée Infection, Marseille, France.

7 2: IHU Méditerranée Infection, Marseille, France.

8 3: CNRS, Marseille, France.

9 *: corresponding author

10

11

12 Keywords: *Treponema*, *Treponema pallidum*, syphilis, ancient genome, pre-Columbian

13

14 **Abstract**

15 Syphilis dramatically hit Europe at the end of the fifteen century before spreading to other
16 continents. Yet the origin of the sudden pandemic in the Old World remains debated, in
17 particular because the leading Columbus hypothesis of a New World origin of historical
18 syphilis in Europe lacks paleomicrobiological confirmation. Here we screened a worldwide
19 set of >1,700 ancient humans and identified ancient *Treponema pallidum* strains in two pre-
20 Columbian child sacrifices from Tlatelolco, Mexico. Over 12,000 *Treponema*-specific reads
21 were recovered to define a novel *Treponema pallidum* ancient population: *Treponema*
22 *pallidum* str. *tlatelolcoensis*. Phylogenetics show that this population displays ancestral
23 features but also bears the genetic building blocks of disease-causing modern *Treponema*
24 *pallidum* subspecies, hence demonstrating how pre-Colombian Americas were the source of
25 worldwide spread of treponematosis.

26 **Introduction**

27 Syphilis started ravaging Europe at the end of the fifteen century^{1, 2} and is still a worldwide
28 disease over five hundred years later, with modern pandemic strains that trace back to a
29 common ancestor in the mid-twentieth century³ having caused an estimated 6.3 million
30 cases in 2016⁴. Although the first complete genome of the syphilis spirochete was
31 characterized 25 years ago⁵, and dozens of additional *Treponema* genomes followed, the
32 antiquity, sources, and dynamics of diffusion of human treponematoses in modern
33 populations in Europe remains uncertain. Part of the challenge is that the *T. pallidum*
34 subspecies that cause venereal syphilis (*T. pallidum* subsp. *pallidum*) and non-venereal yaws
35 (*T. pallidum* subsp. *pertenue*) and bejel (*T. pallidum* subsp. *endemicum*) remain
36 undistinguishable by morphology and antigenicity^{6, 7}, and can only be identified through
37 study of multiple genetic markers and near whole-genome sequencing^{7, 8, 9}. In addition, only
38 a limited number of investigations convincingly yielded ancient *Treponema pallidum*
39 (*T. pallidum*) complex in Europe and Mexico, and none of those could be identified as
40 unambiguously pre-Columbian^{10, 11, 12}. Hence the leading Columbus hypothesis of a New
41 World origin of historical syphilis in Europe^{13, 14} lacks paleomicrobiological confirmation.

42 Here we searched for *Treponema pallidum* strains in a worldwide set of >1,700 ancient
43 human genomes and identified two such cases from 14th-15th century Mexico¹⁵. These
44 ancient genomes prove that *Treponema pallidum* genomes existed in pre-Columbian
45 Americas and provide an unprecedented opportunity to define what role Christopher
46 Columbus' travels played in worldwide spread of syphilis.

47

48

49 **Results**

50 ***Two ancient *Treponema* genomes from pre-Columbian Tlatelolco, Mexico***

51 To search for ancient *Treponema pallidum* genomes, we screened a worldwide set of over
52 1,700 ancient human genomes (Supplementary Figs. 1-2) with five *Treponema*-specific
53 probes (see Methods). Two positive cases were identified in the remains of children who
54 died in Tlatelolco city, Mexico in AD 1325-1520, at ages 4-6 (individuals IF #9 and IF #11 in
55 ref¹⁵). Genomewide investigation isolated over 12,000 unique reads through a stringent 3-
56 step procedure designed to capture all specific *Treponema* reads: 8,922 reads for IF #9 and
57 3,458 reads for IF #11 (Supplementary Fig. 3). The reads displayed the typical features of
58 ancient DNA (Supplementary Fig. 4) and were then mapped against a reference *T. pallidum*
59 genome to cover 38% (428kb; IF #9) and 17% (193kb; IF #11) of that reference (Fig. 1b,d)
60 with a homogenous distribution (Fig. 1a, c).

61

62 ***The Tlatelolco genomes are new members of the *T. pallidum* complex***

63 To investigate the relationships between the two Tlatelolco genomes and other *Treponema*
64 genomes, we first performed a genomewide phylogenetic analysis with the raw sequences
65 using three methods (Fig. 1e). All three methods indicate that the two strains represent a
66 monophyletic group that is a sister group to that formed by *T. pallidum* subsp. *pertenue* and
67 *T. pallidum* subsp. *endemicum*. Yet, the two Tlatelolco genomes appear relatively distinct on
68 the phylogenetic tree and display a raw divergence of ~1.4% (Supplementary Fig. 5). Taking
69 into account the differences that are due to the cytosine deamination of the ancient DNA
70 (Supplementary Fig. 4) cuts this divergence to an estimated maximum of 0.86%

71 (Supplementary Fig. 5). This is still a relatively high level and so it is possible these genomes
72 are indeed distinct despite originating from the same ancient city. Consistent with this
73 possibility, the two genomes display the same differences at 21 positions than those
74 observed between the modern *Trepanoma* genome sequences used in the alignment.

75 Hence the Tlatelolco genomes represent the first two Pre-Columbian sequences of the
76 *T. pallidum* complex. Because they also represent a new clade, we named them *T. pallidum*
77 str. *tlatelolcoensis* #1 (IF #9) and #2 (IF #11).

78

79 ***T. pallidum* str. *tlatelolcoensis* carries distinct phylogenetic signals**

80 To further analyze the *T. pallidum* str. *tlatelolcoensis* sequences, we then focused on just the
81 largest sequence of the two so that the region in common with the other sequences would
82 shift from ~72kb (Fig. 1e) to ~403kb (Fig. 1f). The first noticeable difference is that while the
83 position of the sequence in the phylogenetic tree does not change, phylogenetic support
84 does and increases with two methods (NJ, ML) but decreases with one (parsimony). While
85 this could be just phylogenetic noise, this could also be indicative of underlying divergent
86 signals in the dataset (see comment in methods) and to test this possibility, we did a simple
87 split of the dataset in two halves and analyzed them independently (Supplementary Fig. 6).
88 This analysis shows that for the first half of the dataset (Supplementary Fig. 6a and 6b), the
89 methods diverge significantly, as assessed by a Shimodaira-Hasegawa test of alternative
90 phylogenetic hypotheses that does reject the NJ and parsimony trees (Supplementary
91 Fig. 6d; alpha=0.05).

92 Because visual inspection of the alignment hinted at the presence of divergent signals in
93 different regions, we set to test the homogeneity of the phylogenetic signal by dividing the
94 whole genome into segments. For this analysis, we used windows of 15kb after checking that
95 this would lead to segments with an average of at least 10 differences between the
96 *T. pallidum* subspecies (Supplementary Fig. 7), which should ensure good resolution of the
97 relationships between the groups. Interestingly, this analysis reveals distinct patterns
98 regarding the position of *T. pallidum* str. *tlateolcoensis* comparing to the three modern *T.*
99 *pallidum* strains: for 7 of the 27 segments (~26%), its split is anterior to that of the three
100 subspecies, for another 11 segments (~41%), its split is anterior to that of two the three
101 subspecies, and for four segments (~15%) the split is associated with just one subspecies
102 (Supplementary Fig. 8 and Fig. 2). To confirm this phylogenetic signal, we concatenated the
103 segments with the same individual signal for the three largest groups (Fig. 2). This analysis
104 shows strong and consistent phylogenetic signal between the methods for the position of
105 the *T. pallidum* str. *tlateolcoensis*. To further test this signal, we also conducted Shimodaira-
106 Hasegawa tests of alternative phylogenetic hypotheses (Supplementary Fig. 9) and for two of
107 the three patterns, these tests significantly reject the alternative tree topologies: for the
108 clustering with the two subspecies *T. pallidum* subsp. *pertenue* and *T. pallidum* subsp.
109 *endemicum* ($\alpha=0.001$; Supplementary Fig. 9c) and for the clustering with *T. pallidum*
110 subsp. *pallidum* ($\alpha=0.05$; Supplementary Fig. 9b).

111 This analysis hence shows that *T. pallidum* str. *tlateolcoensis* represents a genome with
112 distinct phylogenetic signals. This pattern is consistent with *T. pallidum* str. *tlateolcoensis*
113 having evolved in pre-Columbian America as part of the ancestral *T. pallidum* population that
114 experienced the transition from a single common ancestor to the three ancestors of the
115 three *T. pallidum* subspecies (Fig. 3).

116 **Discussion**

117 Mexico-Tlatelolco was a pre-Columbian city state built around 1337 on a small island of now
118 dried-up Texcoco's lake. It was regarded as the rival of the ancient capital Mexico-
119 Tenochtitlan after Tlatelolco city developed a merchant empire considered one of the most
120 important centers of activity of Mesoamerica¹⁶. Human sacrifice in pre-Columbian
121 civilizations was highly ritualized and sacrificial inclusion was recently linked to
122 impoverishment and to a high prevalence of infectious diseases¹⁷. It is thus noteworthy that
123 the two children who carried the *T. pallidum* str. *tlateolcoensis* characterized here were
124 sacrificed girls, aged 4-6 years¹⁵, supporting the possibility that they displayed visible signs of
125 the *Treponema* infection.

126

127 In the absence of previously reported paleomicrobiological traces of treponematoses in the
128 New world¹⁴, the cases reported here represent the first genetic evidence of a *T. pallidum*
129 complex species in pre-Columbian America. This result is in agreement with phylogenetic
130 predictions¹⁸ and the observation of Pre-Columbian skeletal lesions characteristic of
131 syphilis¹⁹. Importantly, this result is unambiguous as every single sequence read used for the
132 genome assemblies belonged to the *T. pallidum* complex and the phylogenetic position of
133 the resulting reconstructed genomes within the *T. pallidum* complex is confirmed by simple
134 (NJ, parsimony) and more elaborated (ML) methods, which underlines the clear phylogenetic
135 signal. Finally, while the two reconstructed genomes are incomplete, all analyses were
136 restricted to the segments common to all the genomes used so as to avoid any potential bias
137 due to sequence size differences. Taken together, these data thus clearly demonstrate the
138 presence of a *T. pallidum* complex species in pre-Columbian America.

139

140 The pre-Columbian *T. pallidum* complex species identified in this study are closely related in
141 global phylogenies to the modern *T. pallidum* complex species. In and of itself, this
142 phylogenetic closeness is strong evidence that the two are direct descendants rather than
143 just cousins. Indeed, any evolutionary scenario that would not make them direct
144 descendants would require them to have separated well before the peopling of America,
145 over 10kya²⁰. This ancient split would be inconsistent with recent molecular estimates of the
146 split between the three *T. pallidum* subspecies estimated at ~4.6kya (with 95% highest
147 posterior density intervals of ~6.9-2.6 kya)¹¹. Consistent with this, *T. pallidum* str.
148 *tlateolcoensis* includes both segments that are equivalent to those of two or three of the
149 *T. pallidum* subspecies and segments that are equivalent to those of just one subspecies.
150 This shows that pre-Columbian America is the region of the world where the transition from
151 a single common ancestor to the direct ancestors of the three subspecies occurred. Hence
152 the building blocks that are necessary to form the three *T. pallidum* subspecies were present
153 in this geographical location and time period. 15th century America is thus a required stop on
154 the evolutionary path that led to modern *T. pallidum* subspecies. Notably, the largest group
155 of segments related to just one *Treponema* subspecies in the genome of *T. pallidum* str.
156 *tlateolcoensis* is for *Treponema pallidum* subsp. *pallidum*, the subspecies that causes
157 syphilis. And so, for the syphilis outbreaks to occur in Europe, those ~75kb blocks
158 (Supplementary Fig. 9a) would have had to be brought to Europe. Hence the
159 characterization of *T. pallidum* str. *tlateolcoensis* provides paleomicrobiological support to
160 the hypothesis that Christopher Columbus 'crew returning in Europe in 1493 brought
161 venereal treponematosis to the continent, leading to the 1495 outbreak during the siege of
162 Naples by the army of French King Charles VIII^{2,21}.

163

164 Interestingly, about half of the *T. pallidum* str. *tlateolcoensis* genome has segments that are
165 not related to just one single *T. pallidum* subspecies. While the exact age of the remains is
166 not known and was initially associated with the Pre-Columbian era for this region of the
167 Americas (1325-1520 CE), recent radiocarbon dating for remains excavated in the same
168 locations points at date estimates that fall between 1332 and 1445 CE¹⁷. The strain
169 characterized here may thus have preceded the arrival of Christopher Columbus by 50-150
170 years. Hence the level of differentiation of *T. pallidum* strains in 1492 was more advanced
171 than that observed for *T. pallidum* str. *tlateolcoensis*, and full differentiation between the
172 three *T. pallidum* subspecies likely occurred around the time of Christopher Columbus'
173 travels. This raises interesting questions about how this differentiation is linked to the travels
174 themselves (potential founder effect) or to the impact of encountering a naïve population in
175 Europe.

176

177 **Methods**

178 ***Screening ancient human genomes for *T. pallidum* DNA.***

179 To identify studies that characterized ancient human genomes, we conducted bibliographical
180 searches in Pubmed (<https://pubmed.ncbi.nlm.nih.gov/>) with 'ancient', 'human', 'DNA', and
181 'genomes' keywords. Raw genome data for the identified studies was obtained from the
182 European Nucleotide Archive database (<https://www.ebi.ac.uk/ena/browser/home>). A total
183 of 1,783 genomes from four regions of the world were obtained (Supplementary Figs. 1-2).

184 These ancient genomes were screened *in silico* using a low stringency approach with the
185 Bowtie2 software²² and five probes: one specific to the *Treponema* genus (*flgE*) and four
186 *T. pallidum*-specific ones (*polA*, *tpp47*, *tprL* and *tp0619*)^{8, 9}. Specificity of the isolated reads
187 was assessed through BLAST searches²³ against the National Center for Biotechnology
188 Information (NCBI) non-redundant nucleotide database.

189

190 ***Reconstruction of the *T. pallidum* str. *tlatelolcoensis* genomes.***

191 After two positive cases were identified with our screening probes, we isolated *Treponema*-
192 specific genomewide reads using a 3-step approach (Supplementary Fig. 3). To maximize the
193 likelihood to capture all relevant reads, the first step was the same low stringency approach
194 as that used for the screen with the probes using Bowtie2 software and a complete *T.*
195 *pallidum* reference genome (*T. pallidum* subsp. *pallidum* strain Nichols; NC_021490.2).

196 A filtering stage was then performed, using Kraken2 software²⁴ to assess specificity of the
197 isolated reads and identify the source organisms for the *non-Treponema* reads. Monitoring
198 of the results was performed with Krona software²⁵. References for the five most

199 represented *non-Treponema* genomes were obtained and a specificity analysis was
200 conducted with Bowtie2 to isolate reads that were more related to the *Treponema*
201 reference than to the *non-Treponema* references. Specificity was then reassessed with
202 Kraken and the new five most represented *non-Treponema* genomes were used as negative
203 references for another filtering. This loop was repeated until 25 negative genome references
204 were used and the pool of reads reached 98% specificity for *Treponema*. In all these analyses
205 a tolerance of eight differences comparing to the references was allowed.

206 Finally, to validate the specificity of the reads obtained after step #2, we conducted BLAST
207 searches²³ for each read as a third and final step. Searches were performed using the
208 MEGABLAST program against the bacteria section of the NCBI non-redundant nucleotide
209 database. Reads that produced no hit at this step were analyzed again using the BLASTN
210 program. Reads with a non-*Treponema* best hit were discarded before the assembly step.

211

212 ***Authenticity of ancient DNA.***

213 Authenticity of ancient DNA was verified by investigating for signs of cytosine deamination
214 with mapDamage²⁶ and for signs of DNA fragmentation by assessing read size distribution
215 (Supplementary Fig. 4).

216

217 ***Assembly and consensus.***

218 After filtering, the isolated reads were mapped against a *T. pallidum* subsp. *pallidum* strain
219 Nichols genome sequence (NC_021490.2) using Mira assembly software²⁷. Assemblies were

220 visualized with the gap4 software of the STADEN package²⁸ and a consensus sequence was
221 extracted using a ‘Base frequencies’ algorithm with a 51% cutoff.

222 Representation of the coverage for the genome assembly was performed with Circleator²⁹;
223 in those representations, GC content and gene content is from the reference (*T. pallidum*
224 subsp. *pallidum* strain Nichols).

225

226 ***Phylogenetic analyses.***

227 *Treponema pallidum* str. *tlateolcoensis* genomes were aligned with a representative set of
228 30 complete and modern *Treponema* genome sequences representing the three *T. pallidum*
229 subspecies. Alignment was performed with the MAFFT software³⁰ followed by manual
230 corrections. In all analyses, the columns with alignment gaps or missing information were
231 discarded (complete deletion datasets). Because of this, we did not include other ancient
232 sequences: indeed, when trying to compare our sequences to those of Majander and
233 colleagues¹¹ for example, there was less than 10kb of common sequence.

234 All phylogenetic analyses were conducted with three methods: maximum-likelihood (ML),
235 neighbor-joining (NJ) and parsimony. While ML methods are often the preferred choice over
236 the other two methods, such a combination of simple and more elaborated phylogenetic
237 methods can be helpful to detect underlying issues in the sequence data such as
238 recombination, positions of functional divergence between paralogues, or biases created by
239 outgroups as those issues often lead to incongruence in the results between the methods³¹.

240 NJ phylogenetic analyses were performed with MEGA11³² using the Tamura-Nei method
241 with 500 replicates. PAUP*4.0a169³³ and the tree bisection-reconnection branch swapping

242 algorithm were used for parsimony analyses with 500 replicates and a heuristic search. ML
243 analyses were performed with RAXML8³⁴ under the available model (GTR+gamma) with 500
244 replicates (rapid bootstrapping).

245 Tree topology comparisons were performed using the Shimodaira-Hasegawa test of
246 alternative phylogenetic hypotheses with re-sampling estimated log-likelihood optimization,
247 and 10,000 bootstrap replicates (as implemented in PAUP*4.0b10). This comparison was
248 made with the maximum likelihood model of DNA substitution defined using MODELTEST³⁵
249 and the Akaike information criterion.

250

251 **FIGURE LEGENDS**

252 **Fig. 1.** *Treponema pallidum* str. *tlatelolcoensis* is a basal, pre-Columbian *T. pallidum* strain.
253 (a to d) Characteristics of the *T. pallidum* str. *tlatelolcoensis* genomes from individuals IF #9
254 (a and b) and IF #11 (c and d). (a and c) Circleators plot for the novel genomes with read
255 coverage (internal layer; minimum, average and maximum coverage are given) plotted
256 against GC content (outer layer) and gene content (two middle layers) from the reference
257 (*T. pallidum* subsp. *pallidum* strain *Nichols*). (b and d) Statistics for the genome assemblies.
258 (e and f) *T. pallidum* str. *tlatelolcoensis* is a basal *T. pallidum* strain. Full-genome
259 phylogenetic analysis on the common segments of 32 (e) or 31 (f) *Treponema* genomes using
260 neighbor-joining (NJ), parsimony, and maximum-likelihood (ML) methods. The NJ tree
261 topology was used for the display, with a midpoint rooting. Bootstrap support is given for six
262 (f) or seven (e) nodes (from top to bottom: ML, parsimony, NJ). Circles at nodes indicate
263 bootstrap support of 100 with all methods. *, bootstrap support <50. Black pentagons,
264 *T. paraluisuniculi* outgroup.

265

266 **Fig. 2.** *T. pallidum* str. *tlatelolcoensis* displays distinct phylogenetic patterns in its
267 relationships to modern *T. pallidum* subspecies. The genome sequence of *T. pallidum* str.
268 *tlatelolcoensis* was divided in 27 segments of 15kb each and phylogenetically compared to
269 the corresponding sequences of 30 other *Treponema* genomes using NJ, parsimony, and ML
270 methods (Supplementary Fig. 8). The central bloc summarizes orthology to *T. pallidum* str.
271 *tlatelolcoensis* for each segment using the colour scheme displayed in the bottom left
272 corner. Pal, *T. pallidum* subsp. *pallidum*. End, *T. pallidum* subsp. *endemicum*. Per, *T. pallidum*
273 subsp. *pertenuie*. ‘Concatenated’ phylogenetic analyses were conducted for the three largest

274 groups of segments: results are displayed above and below the central bloc and, together
275 with statistical tests of topologies (Supplementary Fig. 9) confirm that these segments have
276 distinct phylogenetic signals.

277

278 **Fig. 3.** *T. pallidum* str. *tlateolcoensis* belongs to a *Treponema* population that is ancestral to
279 the three modern *T. pallidum* subspecies. The model of evolution has three stages
280 (ancestral, differentiation and recombination, and modern) and uses the same colour
281 scheme and segments as those of Fig. 2. In the upper part of the model is the ancestral
282 *T. pallidum* genome. The central part of the model shows the emergence of the three
283 *T. pallidum* subspecies through differentiation and recombination, as well as the presence of
284 *T. pallidum* str. *tlateolcoensis* in the population, together with two putative variants. The
285 colour scheme uses the modern species as references and may give the impression that
286 modern sequences did not recombine while some, like *T. pallidum* str. *tlateolcoensis* did:
287 this is arbitrary and would require more sequences from the ancestral population to
288 reconstruct how the three modern subspecies were formed.

289

290 **References**

- 291
- 292 1. Crosby AW. The Early History of Syphilis: A Reappraisal. *Am Anthropol* **71**, 218-227 (1969).
- 293
- 294 2. Tognotti E. The rise and fall of syphilis in Renaissance Europe. *J Med Humanit* **30**, 99-113 (2009).
- 295
- 296
- 297 3. Arora N, *et al.* Origin of modern syphilis and emergence of a pandemic *Treponema pallidum* cluster. *Nat Microbiol* **2**, 16245 (2016).
- 298
- 299
- 300 4. Rowley J, *et al.* Chlamydia, gonorrhoea, trichomoniasis and syphilis: global prevalence and incidence estimates, 2016. *Bull World Health Organ* **97**, 548-562P (2019).
- 301
- 302
- 303 5. Fraser CM, *et al.* Complete genome sequence of *Treponema pallidum*, the syphilis spirochete. *Science* **281**, 375-388 (1998).
- 304
- 305
- 306 6. Engelkens HJ, Vuzevski VD, ten Kate FJ, van der Heul P, van der Sluis JJ, Stoltz E. Ultrastructural aspects of infection with *Treponema pallidum* subspecies pertenue (Pariaman strain). *Genitourin Med* **67**, 403-407 (1991).
- 307
- 308
- 309
- 310 7. Giacani L, Lukehart SA. The endemic treponematoses. *Clin Microbiol Rev* **27**, 89-115 (2014).
- 311
- 312 8. Gayet-Ageron A, Combescure C, Lautenschlager S, Ninet B, Perneger TV. Comparison of Diagnostic Accuracy of PCR Targeting the 47-Kilodalton Protein Membrane Gene of *Treponema pallidum* and PCR Targeting the DNA Polymerase I Gene: Systematic Review and Meta-analysis. *J Clin Microbiol* **53**, 3522-3529 (2015).
- 313
- 314
- 315
- 316
- 317 9. Knauf S, *et al.* Gene target selection for loop-mediated isothermal amplification for rapid discrimination of *Treponema pallidum* subspecies. *PLoS Negl Trop Dis* **12**, e0006396 (2018).
- 318
- 319
- 320 10. Giffin K, *et al.* A treponemal genome from an historic plague victim supports a recent emergence of yaws and its presence in 15(th) century Europe. *Sci Rep* **10**, 9499 (2020).
- 321
- 322
- 323 11. Majander K, *et al.* Ancient Bacterial Genomes Reveal a High Diversity of *Treponema pallidum* Strains in Early Modern Europe. *Curr Biol* **30**, 3788-3803 e3710 (2020).
- 324
- 325
- 326 12. Schuenemann VJ, *et al.* Historic *Treponema pallidum* genomes from Colonial Mexico retrieved from archaeological remains. *PLoS Negl Trop Dis* **12**, e0006447 (2018).
- 327
- 328
- 329 13. Beale MA, Lukehart SA. Archaeogenetics: What Can Ancient Genomes Tell Us about the Origin of Syphilis? *Curr Biol* **30**, R1092-R1095 (2020).
- 330
- 331

- 332 14. Harper KN, Zuckerman MK, Harper ML, Kingston JD, Armelagos GJ. The origin and antiquity
333 of syphilis revisited: an appraisal of Old World pre-Columbian evidence for treponemal
334 infection. *Am J Phys Anthropol* **146 Suppl 53**, 99-133 (2011).
- 335
336 15. Morales-Arce AY, McCafferty G, Hand J, Schmill N, McGrath K, Speller C. Ancient
337 mitochondrial DNA and population dynamics in postclassic Central Mexico: Tlatelolco (ad
338 1325–1520) and Cholula (ad 900–1350). *Archaeol Anthropol Sci* **11**, 3459-3475 (2019).
- 339
340 16. *The Oxford encyclopedia of Mesoamerican cultures*. Oxford university press, Oxford New-
341 York (2001).
- 342
343 17. Blevins KE, McGrane M, Mansilla Lory J, Guilliem Arroyo S, Buikstra JE. Structural Violence
344 and Physical Death at Tlatelolco: Selecting the Chronically Malnourished for Sacrifice at a
345 Late Postclassic Mesoamerican City (1300–1521 CE). *Bioarchaeol Int* **7**, 1-31 (2022).
- 346
347 18. Harper KN, *et al.* On the origin of the treponematoses: a phylogenetic approach. *PLoS Negl
348 Trop Dis* **2**, e148 (2008).
- 349
350 19. Tampa M, Sarbu I, Matei C, Benea V, Georgescu SR. Brief history of syphilis. *J Med Life* **7**, 4-10
351 (2014).
- 352
353 20. Willerslev E, Meltzer DJ. Peopling of the Americas as inferred from ancient genomics. *Nature*
354 **594**, 356-364 (2021).
- 355
356 21. Baker BJ, Armelagos GJ. The origin and antiquity of syphilis: paleopathological diagnosis and
357 interpretation. *Curr Anthropol* **29**, 703-738 (1988).
- 358
359 22. Langmead B, Salzberg SL. Fast gapped-read alignment with Bowtie 2. *Nat Methods* **9**, 357-
360 359 (2012).
- 361
362 23. Altschul SF, *et al.* Gapped BLAST and PSI-BLAST: a new generation of protein database search
363 programs. *Nucleic Acids Res* **25**, 3389-3402 (1997).
- 364
365 24. Wood DE, Salzberg SL. Kraken: ultrafast metagenomic sequence classification using exact
366 alignments. *Genome Biol* **15**, R46 (2014).
- 367
368 25. Ondov BD, Bergman NH, Phillippy AM. Interactive metagenomic visualization in a Web
369 browser. *BMC Bioinformatics* **12**, 385 (2011).
- 370
371 26. Jonsson H, Ginolhac A, Schubert M, Johnson PL, Orlando L. mapDamage2.0: fast approximate
372 Bayesian estimates of ancient DNA damage parameters. *Bioinformatics* **29**, 1682-1684
373 (2013).

- 374
- 375 27. Chevreux B, *et al.* Using the miraEST assembler for reliable and automated mRNA transcript
- 376 assembly and SNP detection in sequenced ESTs. *Genome Res* **14**, 1147-1159 (2004).
- 377
- 378 28. Staden R, Beal KF, Bonfield JK. The Staden package, 1998. *Methods Mol Biol* **132**, 115-130
- 379 (2000).
- 380
- 381 29. Crabtree J, Agrawal S, Mahurkar A, Myers GS, Rasko DA, White O. Circleator: flexible circular
- 382 visualization of genome-associated data with BioPerl and SVG. *Bioinformatics* **30**, 3125-3127
- 383 (2014).
- 384
- 385 30. Katoh K, Standley DM. MAFFT multiple sequence alignment software version 7:
- 386 improvements in performance and usability. *Mol Biol Evol* **30**, 772-780 (2013).
- 387
- 388 31. Abi-Rached L, Gilles A, Shiina T, Pontarotti P, Inoko H. Evidence of en bloc duplication in
- 389 vertebrate genomes. *Nat Genet* **31**, 100-105 (2002).
- 390
- 391 32. Tamura K, Stecher G, Kumar S. MEGA11: Molecular Evolutionary Genetics Analysis Version
- 392 11. *Mol Biol Evol* **38**, 3022-3027 (2021).
- 393
- 394 33. Swofford DL. PAUP*: Phylogenetic analysis using parsimony (*and other methods), version
- 395 4.0. (eds. Sinauer, Sunderland, Massachusetts (2001).
- 396
- 397 34. Stamatakis A. RAxML version 8: a tool for phylogenetic analysis and post-analysis of large
- 398 phylogenies. *Bioinformatics* **30**, 1312-1313 (2014).
- 399
- 400 35. Posada D, Crandall KA. MODELTEST: testing the model of DNA substitution. *Bioinformatics*
- 401 **14**, 817-818 (1998).
- 402
- 403
- 404

405 **Acknowledgements**

406 M.G. benefited a Master grant from Fondation Méditerranée Infection, Marseille, France.

407

408 **Author contributions**

409 M.D initiated the study. M.D and L.A-R designed and supervised the study. M.G conducted
410 the study. M.G. and L.A-R performed the analyses. All authors worked on the data analysis
411 and interpretation and wrote the manuscript.

412

413 **Competing interests**

414 The authors declare no competing interest.

415

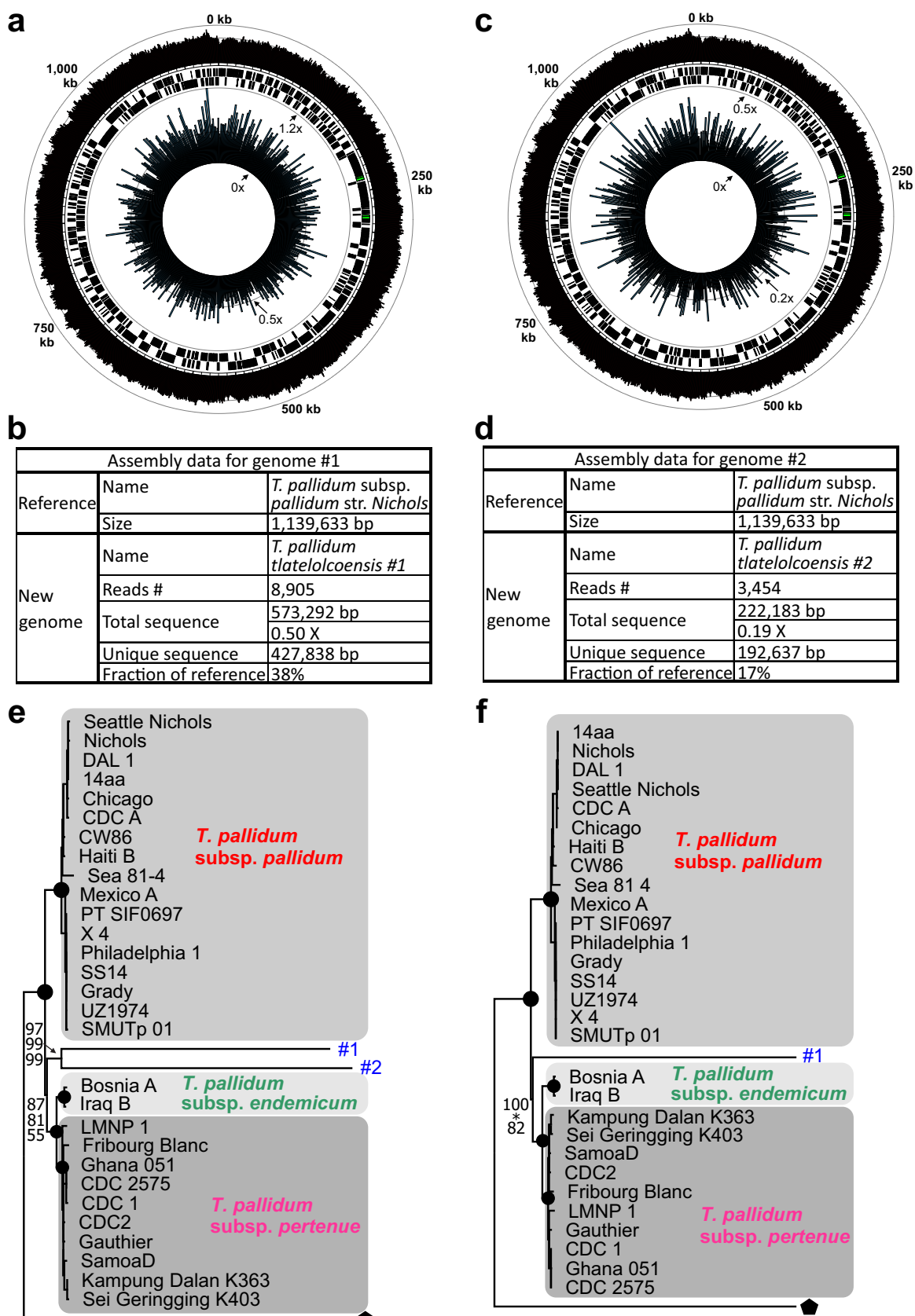


Fig. 1

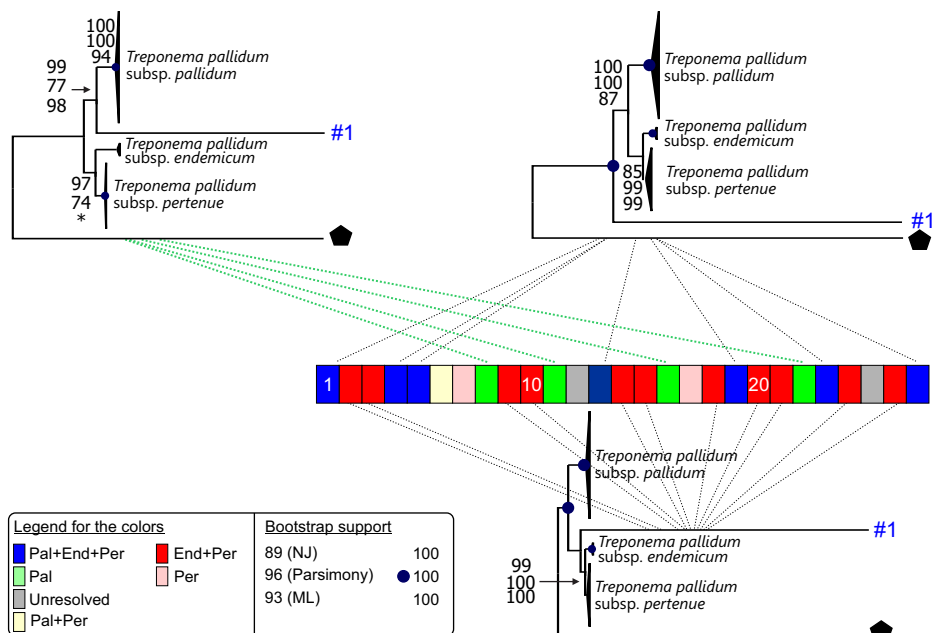


Fig. 2

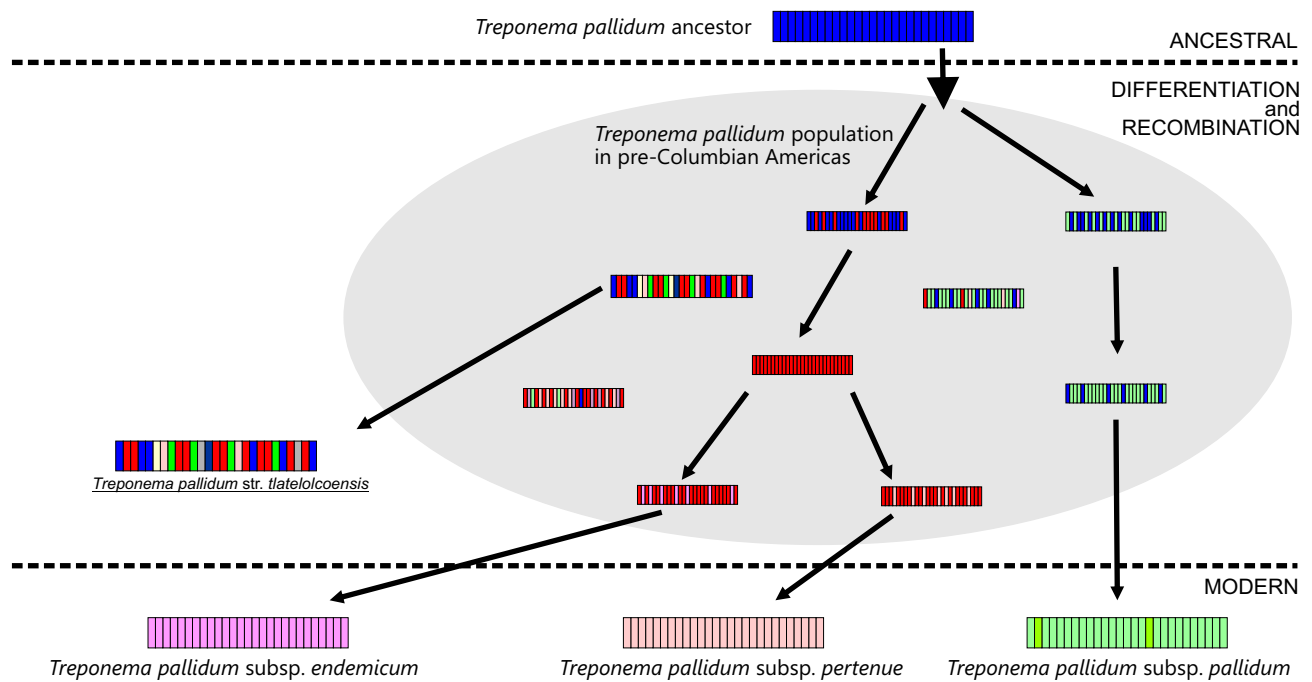


Fig. 3